

High-throughput Screening of Compounds against Autoluminescent Nonreplicating *Mycobacterium tuberculosis* under Diverse Conditions

Xirong Tian ^{a,b,c,d*}, Wanli Ma ^{a,b,c,d*}, Buhari Yusuf ^{a,b,c,d}, Chunyu Li ^{a,b,c,d}, H.M. Adnan

Hameed ^{a,b,c,d}, Xinyue Wang ^{e,f}, Nanshan Zhong ^e, Jinxing Hu ^{f#}, Tianyu Zhang ^{a,b,c,d,f#}

^a State Key Laboratory of Respiratory Disease, Guangzhou Institutes of Biomedicine

and Health (GIBH), Chinese Academy of Sciences (CAS), Guangzhou 510530, China

^b Guangdong-Hong Kong-Macao Joint Laboratory of Respiratory Infectious Diseases,

Guangzhou Institutes of Biomedicine and Health (GIBH), Chinese Academy of

Sciences (CAS), Guangzhou 510530, China

^c University of Chinese Academy of Sciences (UCAS), Beijing 100049, China

^d China-New Zealand Joint Laboratory on Biomedicine and Health, Guangzhou

Institutes of Biomedicine and Health, Chinese Academy of Sciences, Guangzhou

510530, China

^e Guangzhou National Laboratory, Guangzhou 510005, China

^f Guangzhou Chest Hospital, Guangzhou 510005, China

*These authors contributed equally to this work.

#Corresponding author:

Tianyu Zhang, Tel: +86-20-32015270, E-mail: zhang_tianyu@gibh.ac.cn

Jinxing Hu, Tel: +86-20-83594895, E-mail: hujinxing2000@163.com

1 **KEYWORDS**

2 Autoluminescence; Low-oxygen; Persistence; *Mycobacterium tuberculosis*; High-
3 throughput screening

4 **ABSTRACT**

5 The screening of new anti-mycobacterial chemicals is primarily focused on inhibiting
6 the active growing bacteria. However, a major challenge in tuberculosis control is the
7 ability of *Mycobacterium tuberculosis* to enter a nonreplicating state for extended
8 periods, rendering it resistant to many clinical drugs and complicating eradication
9 efforts. Existing low-oxygen-recovery assays designed for screening compounds
10 targeting nonreplicating *M. tuberculosis* have limitations, including the colony-
11 forming unit counting for non-luminous *M. tuberculosis* and the instability of the free
12 plasmid carrying *luxAB* genes in luminescent *M. tuberculosis*, along with exogenous
13 substrate requirements for light producing. Moreover, these assays fail to accurately
14 replicate the growth conditions of nonreplicating *M. tuberculosis* *in vitro*, thus
15 resulting in less convincing results. To address these challenges, we have developed
16 an autoluminescence-based, cholesterol-enriched culture evaluation model to assess
17 17 anti-tuberculosis drugs of different classes against nonreplicating *M. tuberculosis*.
18 Our findings indicate that the relative light unit, measured in real-time, serves as a
19 reliable surrogate marker for colony-forming unit, which typically becomes available
20 one month later. This suggests the utility of our model for the rapid determination of
21 drug susceptibility dynamically. The autoluminescent *M. tuberculosis*, harbouring
22 *luxCDABE* gene cluster within its genome, can emit blue-green light stably and
23 autonomously without requiring an external substrate supplement. The minimal
24 inhibitory concentrations of all the drugs tested under anaerobic conditions are
25 significantly different from that detected in aerobic environment. Our model allows

26 for rapid, precise, and efficient assessment of drug activity under anaerobic conditions,
27 thereby enabling a more comprehensive evaluation of anti-mycobacterial efficacy.
28 Overall, our model represents a significant advancement in anti-tuberculosis drug
29 discovery and pharmaceutical development.

30 INTRODUCTION

31 The highly infectious pathogen *Mycobacterium tuberculosis* is the causative
32 agent of tuberculosis (TB), and was responsible for 10.6 million TB individuals
33 globally in 2022 (1). The emergence of drug-resistant *M. tuberculosis* strains, coupled
34 with lethal coinfections with human immunodeficiency virus, has significantly
35 exacerbated the global healthcare crisis, necessitating the exploration of novel drugs
36 or treatment regimens against *M. tuberculosis* (2, 3). Notably, after four decades of
37 persistent efforts, bedaquiline (BDQ), the first new anti-TB medication, received
38 approval from the United States Food and Drug Administration in 2012 (4-6).

39 The persistence of nonreplicating *M. tuberculosis* within lung lesions, capable of
40 surviving for decades and adapting to hypoxic conditions, poses a formidable
41 challenge to TB eradication (7-9). A comprehensive understanding of the complex
42 host environment in which *M. tuberculosis* resides is crucial for developing effective
43 control strategies (10). Previous studies have revealed *M. tuberculosis*'s ability to
44 exploit host-derived cholesterol as a primary carbon source during infection (11). By
45 incorporating cholesterol into growth media, it is more accurately replicate the growth
46 environment of nonreplicating *M. tuberculosis* compared to traditional glycerol-
47 enriched media.

48 Despite the availability of well-established *in vitro* low-oxygen-recovery assays
49 for assessing evaluate drug efficacy against nonreplicating *M. tuberculosis*, these
50 methods still have certain limitations (12-14). Some methods rely on enumerating
51 colony forming units (CFUs) or visible bacterial growth, requiring several months for
52 the completion of testing. Others have employed a luminescent *M. tuberculosis* strain
53 with a free plasmid carrying *luxAB* genes to screen for chemical agents against
54 nonreplicating mycobacteria (6). However, this approach is not favored due to its

55 dependence on additional substrates and the instability of the plasmid (6). Our
56 research introduces an autoluminescence-based, low-oxygen, and cholesterol-enriched
57 evaluation model that utilizes autoluminescent *M. tuberculosis* H37Ra (AlRa),
58 emitting stable and efficient blue-green light dynamically over an extended period
59 without requiring substrate supplementation. Bacterial growth is quantified
60 dynamically by measuring relative light units (RLUs) at various time points during
61 the recovery process. In conclusion, our model is designed to be straightforward,
62 time-efficient, labor- and resource-effective, while also facilitating high-throughput
63 screening of drugs and drug combinations against nonreplicating *M. tuberculosis*.

64 **RESULTS**

65 **MICs determination using glycerol- and cholesterol-enriched media under**
66 **aerobic conditions.** Seventeen anti-TB drugs from distinct classes were selected for
67 this study. Cholesterol serves as a primary carbon source during *M. tuberculosis*
68 infection, mimicking the nutritional conditions encountered during the course of *M.*
69 *tuberculosis* infection. Moreover, under aerobic conditions, the minimal inhibitory
70 concentrations (MICs) of the drugs against *M. tuberculosis* remained largely
71 consistent, irrespective of whether glycerol or cholesterol was used as the carbon
72 source. An exception to this was observed with para-aminosalicylic acid (PAS), as
73 detailed in Table 1 and Figure 1. In the glycerol-enriched medium, the MIC of PAS
74 ranged from 0.25 to 1 μ g/mL, however, it increased dramatically to over 64 μ g/mL in
75 the cholesterol-enriched medium (Table 1). The growth curves of actively growing
76 AlRa treated with nine drugs from different categories are shown in Figure 1, and
77 those treated with the remaining eight drugs are shown in Figure S1.

78 **MICs determination using glycerol- and cholesterol-enriched media under**
79 **anaerobic conditions.** We systematically evaluated 17 anti-TB drugs targeting

80 various crucial aspects of *M. tuberculosis* metabolism, including the cell wall, RNA
81 polymerase, ribosome and respiration. Our findings revealed that the MICs of these
82 drugs against *M. tuberculosis* were generally higher under anaerobic conditions
83 compared to aerobic conditions with the exception of rifampin (RIF) and rifabutin
84 (RFB), as depicted in Table 1, Figures 2 and Figure S2. Additionally, the MICs of the
85 drugs remained relatively consistent under anaerobic conditions, regardless of
86 whether the medium was supplemented with glycerol or cholesterol, with the
87 exception of moxifloxacin (MOX). The MICs of MOX against nonreplicating *M.*
88 *tuberculosis* were found to be in the range of 0.125-2 μ g/mL in the presence of
89 glycerol, whereas in the presence of cholesterol, the MICs spanned from 8-32 μ g/mL
90 (Table 1). Both MOX and levofloxacin (LEV), the two fluoroquinolones, exhibited
91 increased MICs under anaerobic conditions, regardless of the presence of cholesterol
92 or glycerol in the media. Remarkably, MOX displayed a greater efficacy compared to
93 LEV under both anaerobic and aerobic conditions.
94 Under anaerobic conditions, drugs targeting the cell wall, such as vancomycin (VAN),
95 isoniazid (INH), ethambutol (EMB), and ethionamide (ETH), did not display
96 significant antibacterial activity against nonreplicating *M. tuberculosis* as the MICs
97 were over 64 μ g/mL (Table 1). In contrast, these drugs exhibited notable efficacy
98 against actively growing *M. tuberculosis* under aerobic conditions.
99 Compared to other anti-TB drugs, drugs targeting RNA polymerase showed lower
100 MICs with notably effective anti-*M. tuberculosis* activity in both conditions,
101 particularly under anaerobic conditions. The MICs of RIF ranged from 0.0625 to
102 0.125 μ g/mL and 0.125 to 2 μ g/mL under aerobic and anaerobic conditions
103 respectively (Table 1). RFB displayed enhanced efficacy compared to RIF against
104 nonreplicating *M. tuberculosis*, with the MICs as low as 0.03125 to 0.125 μ g/mL and

105 0.03125 to 0.0625 $\mu\text{g}/\text{mL}$ in glycerol- and cholesterol-enriched media, respectively
106 (Table 1). These findings emphasized the promising efficacy of RIF and RFB as
107 candidates for eradicating nonreplicating *M. tuberculosis*, thus establishing a robust
108 foundation for their clinical application.

109 The ribosome-targeting drugs, amikacin (AMK) and streptomycin (STR),
110 demonstrated anti-TB activity against both actively growing and nonreplicating *M.*
111 *tuberculosis*. However, the MICs against nonreplicating *M. tuberculosis* were
112 significantly higher in comparison to those observed against actively growing *M.*
113 *tuberculosis*. Pyrazinoic acid (POA), the active form of pyrazinamide, showed no
114 anti-*M. tuberculosis* activity under anaerobic conditions, with the MIC 800 $\mu\text{g}/\text{mL}$.
115 Under anaerobic conditions, drugs targeting folic acid synthesis exhibited no evident
116 anti-*M. tuberculosis* activity. The MIC of PAS ranged from 0.25-1 $\mu\text{g}/\text{mL}$ in glycerol-
117 enriched 7H9 medium under aerobic conditions, which significantly increased to over
118 64 $\mu\text{g}/\text{mL}$ in cholesterol-enriched 7H9 medium under both aerobic and anaerobic
119 conditions (Table 1).

120 Pretomanid (PA-824) demonstrated pronounced anti-*M. tuberculosis* activity,
121 particularly under anaerobic conditions and with cholesterol as the primary carbon
122 source, with a MIC range of 1-4 $\mu\text{g}/\text{mL}$ (Table 1). TB47 exhibited remarkable anti-*M.*
123 *tuberculosis* activity at an exceptionally low concentration of 0.004 $\mu\text{g}/\text{mL}$ under
124 aerobic conditions (Table 1). However, its efficacy against *M. tuberculosis* became
125 evident only when the concentration was increased to 0.0625-0.25 $\mu\text{g}/\text{mL}$ under
126 anaerobic conditions (Table 1). The MICs of BDQ were 0.5-1 $\mu\text{g}/\text{mL}$ and 1-2 $\mu\text{g}/\text{mL}$
127 against actively growing *M. tuberculosis* when cultivated with glycerol or cholesterol,
128 respectively (Table 1). Nevertheless, under anaerobic conditions, these MICs
129 increased to 4-8 $\mu\text{g}/\text{mL}$ and 4-16 $\mu\text{g}/\text{mL}$ with glycerol or cholesterol, respectively

130 (Table 1). Clofazimine (CLO) exhibited MICs against nonreplicating *M. tuberculosis*
131 ranging from 2-16 µg/mL, significantly higher than those observed against actively
132 growing *M. tuberculosis*, which had an MIC range of 0.5-2 µg/mL (Table 1).

133 **The combined effect of TB47 and CLO against nonreplicating AIRa.** Our results
134 indicated that the combination of TB47 and CLO exhibited partial synergy in terms of
135 sterilizing activity against nonreplicating *M. tuberculosis* under anaerobic conditions,
136 both with glycerol and cholesterol-enriched media with a Fractional Inhibitory
137 Concentration Index (FICI) of 0.75 (Table 2). Notably, the MIC of CLO decreased
138 from 8 to 4 µg/mL in the presence of TB47 at one-fourth of its MIC. These results
139 highlighted the potential of this drug combination for clinical evaluation against
140 nonreplicating *M. tuberculosis*, which has been proved to have strong sterilizing
141 activities against *M. tuberculosis* in a well-established mouse model in two studies
142 carried out by us, and the manuscript of another study is in revision in Antimicrobial
143 Agents and Chemotherapy (15-17). Moreover, the assessment model established in
144 this study for evaluating the efficacy of drug combinations against nonreplicating *M.*
145 *tuberculosis* showed significant promise for informing future research and testing
146 endeavors in this field.

147 **DISCUSSION**

148 During TB infection, *M. tuberculosis* transitions into a nonreplicating state, becoming
149 resistant to many clinical antibiotics and significantly prolonging therapy (18). *M.*
150 *tuberculosis* can acquire and metabolize essential host-derived lipids, particularly
151 cholesterol, which facilitates disease initiation and progression (19). This necessitates
152 the establishment of a representative model that faithfully replicates the growth
153 conditions of nonreplicating *M. tuberculosis* within the host environment. This model
154 is characterized by oxygen deprivation and cholesterol enrichment of growth medium,

155 with the goal of screening for effective drugs against nonreplicating *M. tuberculosis*.

156 To fulfill this objective, we employed AlRa, a strain preserved in our laboratory, to
157 establish an autoluminescence-based drug efficacy evaluation model for high-
158 throughput screening of compounds against nonreplicating *M. tuberculosis*. The RLUs
159 emitted by AlRa, producing blue-green light, exhibit a strong correlation with CFUs,
160 thus serving as a surrogate marker rather than CFUs for quantifying *M. tuberculosis*
161 numbers in culture (20).

162 During the establishment of our model, a notable increase in the growth rate of *M.*
163 *tuberculosis* was observed in cholesterol-enriched medium compared to glycerol-
164 enriched medium, both continuous cultivation under aerobic conditions and recovery
165 after cultivation under anaerobic conditions. This observation supports previous
166 studies suggesting that cholesterol serves as the primary carbon source during *M.*
167 *tuberculosis* infection (11). Our findings suggested that RIF, RFB, PA-824, and TB47
168 demonstrated relatively significant potential for inhibiting nonreplicating *M.*
169 *tuberculosis* under anaerobic conditions, as previously documented (21-23).

170 Conversely, drugs targeting the mycobacterial cell wall, such as INH, EMB, ETH, and
171 VAN, showed negligible anti-mycobacterial activity under anaerobic conditions,
172 consistent with prior published studies (12, 24). The resistance of nonreplicating *M.*
173 *tuberculosis* to these drugs was attributed to the slowed process of cellular division
174 under anaerobic condition. Drugs that target folic acid synthesis, such as
175 sulfamethoxazole (SMX) and PAS, manifested minimal bactericidal activities against
176 nonreplicating *M. tuberculosis* (Table 1). PAS also showed limited activity against
177 actively growing *M. tuberculosis* with a MIC exceeding 64 µg/mL, when applying the
178 media supplemented with cholesterol. As a prodrug activated through the folate
179 synthesis pathway, PAS can be converted into folate intermediate analogs, thereby

180 disrupting *M. tuberculosis*'s folate metabolism (25, 26). It has been hypothesized that
181 the addition of cholesterol, which prevents PAS from entering *M. tuberculosis*, or the
182 unique mechanism of action of PAS, contributes to its ineffectiveness against *M.*
183 *tuberculosis* under cholesterol-enriched media. Ribosome-targeting drugs, AMK and
184 STR, exhibited superior activity against nonreplicating *M. tuberculosis* compared to
185 cell wall-targeting drugs (Table 1). The results are consistent with the observations of
186 some Chinese clinicians, who have noted good treatment efficacy in multi-drug
187 resistant TB patients treated with AMK. This suggests that AMK possesses relatively
188 potent activity in controlling *M. tuberculosis* persisters, despite injection is one of its
189 disadvantages. The MIC of POA against nonreplicating *M. tuberculosis* exceeded 800
190 $\mu\text{g/mL}$. We speculated that anaerobic environment might influence the membrane
191 potential of *M. tuberculosis*, which may contribute to its resistance to POA (27).
192 Generally, MICs of some drugs against nonreplicating *M. tuberculosis* were generally
193 higher than those against actively growing *M. tuberculosis*, indicating that some drugs
194 clinically effective against actively growing *M. tuberculosis* may not effectively treat
195 nonreplicating *M. tuberculosis* in lung lesions, which is demonstrated clearly in
196 animal work (16, 28). It is noteworthy that fluoroquinolones (either LEV or MOX)
197 have not shown significant effects on persisting *M. tuberculosis* in previous animal
198 studies, which is consistent with the predictions made in this study (16, 28). The
199 combination of TB47 and CLO demonstrated promising partial synergistic activity
200 with a FICI as low as 0.75 under anaerobic conditions (Table 2), which supports the
201 finding observed in the animal studies and is promising for clinical trial (15, 16).
202 The model developed in this study for assessing drug activity against nonreplicating
203 *M. tuberculosis* possesses several notable advantages. Firstly, this method stimulates
204 the growth conditions of nonreplicating *M. tuberculosis* within the human host by

205 utilizing media supplemented with cholesterol, thereby ensuring maximal fidelity to
206 the natural environment of the pathogen. Secondly, the model offers simple
207 manipulation as AlRa consistently emits blue-green light without requiring additional
208 substrate aldehyde, thereby guaranteeing stable and consistent results. Thirdly, the
209 results are easily visualized through the consistent detection and comparison of RLU
210 emitted by AlRa at various time intervals. Further exploration should prioritize high-
211 throughput screening of prospective compounds and treatment regimens against
212 nonreplicating *M. tuberculosis* using the current model. In summary, this model holds
213 significant application value and possesses high potential to accelerate the discovery
214 and development of new drugs and treatment strategies targeting nonreplicating *M.*
215 *tuberculosis*, which may closely mirror the real state of *M. tuberculosis* persisters *in*
216 *vivo*.

217 MATERIALS AND METHODS

218 **Mycobacterial strains and culture conditions.** The mycobacterial strain utilized in
219 this study is AlRa, an autoluminescent *M. tuberculosis* H37Ra, which has been
220 genetically engineered to incorporate the *luxCDABE* gene cluster into its genome (20).
221 AlRa emits blue-green light continuously catalyzed by LuxAB (bacterial luciferase)
222 and facilitated by LuxCDE (fatty acid reductase complex), which consistently supply
223 the necessary substrate aldehyde in a recycling form, thereby obviating the need for
224 external substrate supplementation (20). Notably, the drug susceptibility and growth
225 rate of AlRa do not significantly differ from those of the wild type *M. tuberculosis*
226 H37Ra (20). AlRa was cultured at 37°C in Middlebrook 7H9 broth (Difco, Detroit, MI,
227 USA) supplemented with 10% oleic acid-albumin-dextrose-catalase enrichment (BBL,
228 Sparks, MD, USA), 0.2% glycerol, and 0.05% Tween 80.

229 **Antimicrobials.** All pharmaceutical drugs, including ETH, INH, VAN, RIF, RFB,

230 AMK, STR, MOX, LEV, PA-824, SMX, PAS, POA, BDQ, and CLO, were purchased
231 from Meilun (Dalian, China) with a minimum purity threshold of \geq 95%. Additionally,
232 TB47 was synthesized and sent to us as a gift by Boji (Guangzhou, China). AMK,
233 INH, and STR were solubilized in sterilized water, while the remaining drugs were
234 dissolved in dimethyl sulfoxide (DMSO) obtained from Xilong (Shanghai, China). All
235 drug solutions were freshly prepared and stored at 4 $^{\circ}$ C until use.

236 **Chemotherapy under aerobic condition.** The AlRa were cultured in 7H9 medium
237 supplemented with Tween80 at 37 $^{\circ}$ C until the optical density, measured at a
238 wavelength of 600 nm, reached to 0.6-0.8 and the RLU s /mL reached 5 million. The
239 various drug solutions (4 μ L each) were combined with AlRa culture (196 μ L, 10-fold
240 diluted using 7H9 without Tween80 and supplemented with either glycerol or
241 cholesterol) in a sterilized tube and mixed thoroughly. Negative controls were
242 prepared using DMSO and sterilized water. Each drug concentration and negative
243 control were assayed simultaneously in three 1.5 mL EP tubes. The AlRa-drug
244 mixtures underwent a five-day incubation period, during which the RLU s were
245 consistently assessed at identical intervals each day. The MIC_{lux} (MIC based on the
246 detection of autoluminescence) of drugs against the actively growing AlRa is defined
247 as the lowest concentration at which the RLU s in the experimental group are equal to
248 or less than 10% of the RLU s in the control group after 5 days.

249 **Culture of nonreplicating AlRa.** The AlRa strains were cultured until they reached
250 an optical density of 0.6-0.8, measured at a wavelength of 600 nm, and a state of
251 5×10^6 RLU s /mL. Subsequently, the AlRa culture was then transferred to a low-
252 oxygen cabinet (HUAPO, Guangzhou, China) that had already achieved a steady state.
253 This cabinet was programmed to maintain specific conditions, including a temperature
254 of 37 $^{\circ}$ C, an oxygen content of 0.8%, and a carbon dioxide concentration of 5%. The

255 methylene blue solution was then added to the AlRa culture to achieve a final
256 concentration of 6 μ g/mL (29, 30). The cultures were incubated until the blue color
257 disappeared, typically observed within 7-10 days after the addition of methylene blue.

258 **Drug susceptibility tested under anaerobic condition.** Under hypoxic conditions,
259 various drug solutions (4 μ L each) were combined with nonreplicating AlRa culture
260 (196 μ L, 10-fold diluted using 7H9 without Tween80 and supplemented with glycerol
261 or cholesterol) in a sterile tube and mixed thoroughly. The AlRa-drug mixture was
262 then incubated for seven days. To remove any potential carryover effects of residual
263 drugs during the subsequent recovery process, activated carbon (in a volume ratio of
264 1:5, 50 μ L into 200 μ L) was added (15). The tubes were subsequently transferred to a
265 standard aerobic incubator. The RLUs in the co-incubated 1.5 mL EP tubes were
266 measured and recorded at 7-hour intervals over a period of 28 hours. The
267 experimental procedure was repeated three times.

268 **Combined activity assay of TB47 and CLO against nonreplicating AlRa.** Previous
269 research from our group has demonstrated that the combined administration of TB47
270 and CLO significantly exhibits anti-replicating *M. tuberculosis* activity both *in vitro*
271 and *in vivo* (16). In this study, we aim to determine whether this combination would
272 also display notable efficacy against nonreplicating *M. tuberculosis* using the
273 checkerboard method. Specifically, 2 μ L of TB47, 2 μ L of CLO, and 196 μ L of
274 diluted AlRa culture in a nonreplicating state were simultaneously added to the same
275 1.5 mL tube. To eliminate any potential carryover effects of the drugs following seven
276 days of coincubation, activated carbon (at a volume ratio of 1:5, 50 μ L into 200 μ L)
277 was utilized (26). Subsequently, the tubes containing the co-culture were transferred
278 to aerobic conditions, and RLUs were then detected at 7-hour intervals for the
279 following 28 hours. The FICI was calculated as the ratio of the MIC of TB47 in

280 combination to the MIC of TB47 alone, plus the MIC of CLO in combination to the
281 MIC of CLO alone (31). The effects were categorized based on the FICI into five
282 groups: synergistic ($FICI \leq 0.5$), partially synergistic ($0.5 < FICI < 1.0$), additive
283 ($FICI = 1.0$), irrelevant ($1.0 < FICI \leq 4.0$), and antagonistic ($FICI > 4.0$) (31).

284 **Statistical analysis.** Before performing statistical analysis, the RLU values were
285 transformed into their logarithmic counts. The time-kill curves were graphically
286 depicted using GraphPad Prism version 8.3.0.

287 **ACKNOWLEDGMENTS**

288 This work received support from the National Key R&D Program of China
289 (2021YFA1300904), the National Natural Science Foundation of China
290 (21920102003) and by the Guangzhou Science and Technology Planning Project
291 (2023A03J0992). The funders had no role in study design, data collection and
292 analysis, decision to publish, or preparation of the manuscript.

293 **AUTHOR CONTRIBUTIONS**

294 Conceived the project: Tianyu Zhang, Xirong Tian, Wanli Ma, Nanshan Zhong;
295 Designed the research: Tianyu Zhang, Xirong Tian, Wanli Ma, Xinyue Wang, Jinxing
296 Hu, Nanshan Zhong; Performed the studies: Xirong Tian, Wanli Ma, Chunyu Li,
297 Xinyue Wang; Interpreted the results: Tianyu Zhang, Xirong Tian, Wanli Ma, Jinxing
298 Hu; Drafted the manuscript: Tianyu Zhang, Xirong Tian, Wanli Ma, Buhari Yusuf,
299 H.M. Adnan Hameed; Final approval of the manuscript: all authors.

300 **REFERENCES**

301 1. World Health Organization (WHO). 2023. Global Tuberculosis Report.
302 Available at: <https://iris.who.int/bitstream/handle/10665/373828/9789240083851-eng.pdf?sequence=1>
303
304 2. Sala C, Dhar N, Hartkoorn RC, Zhang M, Ha YH, Schneider P, Cole ST. 2010.

305 Simple model for testing drugs against nonreplicating *Mycobacterium*
306 *tuberculosis*. *Antimicrob Agents Chemother* 54:4150-4158.

307 3. Koch A, Mizrahi V. 2018. *Mycobacterium tuberculosis*. *Trends Microbiol*
308 26:555-556.

309 4. Volynets GP, Tukalo MA, Bdzhola VG, Derkach NM, Gumeniuk MI,
310 Tarnavskiy SS, Starosyla SA, Yarmoluk SM. 2019. Benzaldehyde
311 thiosemicarbazone derivatives against replicating and nonreplicating
312 *Mycobacterium tuberculosis*. *J Antibiot (Tokyo)* 72:218-224.

313 5. Kadura S, King N, Nakhoul M, Zhu H, Theron G, Köser CU, Farhat M. 2020.
314 Systematic review of mutations associated with resistance to the new and
315 repurposed *Mycobacterium tuberculosis* drugs bedaquiline, clofazimine,
316 linezolid, delamanid and pretomanid. *J Antimicrob Chemother* 75:2031-2043.

317 6. He W, Liu C, Liu D, Ma A, Song Y, He P, Bao J, Li Y, Zhao B, Fan J, Cheng Q,
318 Zhao Y. 2021. Prevalence of *Mycobacterium tuberculosis* resistant to
319 bedaquiline and delamanid in China. *J Glob Antimicrob Resist* 26:241-248.

320 7. Srivastava S, Cirrincione KN, Deshpande D, Gumbo T. 2020. Tedizolid,
321 faropenem, and moxifloxacin combination with potential activity against
322 nonreplicating *Mycobacterium tuberculosis*. *Front Pharmacol* 11:616294.

323 8. Wayne LG, Sohaskey CD. 2001. Nonreplicating persistence of *mycobacterium*
324 *tuberculosis*. *Annu Rev Microbiol* 55:139-163.

325 9. Iacobino A, Piccaro G, Giannoni F, Mustazzoli A, Fattorini L. 2017. Fighting
326 tuberculosis by drugs targeting nonreplicating *Mycobacterium tuberculosis*
327 bacilli. *Int J Mycobacteriol* 6:213-221.

328 10. Wipperman MF, Sampson NS, Thomas ST. 2014. Pathogen roid rage:
329 cholesterol utilization by *Mycobacterium tuberculosis*. *Crit Rev Biochem Mol*

330 *Biol* 49:269-293.

331 11. Moopanar K, Nyide ANG, Senzani S, Mvubu NE. 2023. Clinical strains of
332 *Mycobacterium tuberculosis* exhibit differential lipid metabolism-associated
333 transcriptome changes in *in vitro* cholesterol and infection models. *Pathog Dis*
334 81:ftac046.

335 12. Cho SH, Warit S, Wan B, Hwang CH, Pauli GF, Franzblau SG. 2007. Low-
336 oxygen-recovery assay for high-throughput screening of compounds against
337 nonreplicating *Mycobacterium tuberculosis*. *Antimicrob Agents Chemother*
338 51:1380-1385.

339 13. Cho S, Lee HS, Franzblau S. 2015. Microplate Alamar blue assay (MABA)
340 and low oxygen recovery assay (LORA) for *Mycobacterium tuberculosis*.
341 *Methods Mol Biol* 1285:281-292.

342 14. Macabeo APG, Vidar WS, Chen X, Decker M, Heilmann J, Wan B, Franzblau
343 SG, Galvez EV, Aguinaldo MAM, Cordell GA. 2011. *Mycobacterium*
344 *tuberculosis* and cholinesterase inhibitors from Voacanga globosa. *Eur J Med
345 Chem* 46:3118-3123.

346 15. Yu W, Yusuf B, Wang S, Tian X, Hameed HMA, Lu Z, Chiwala G, Alam MS,
347 Cook GM, Maslov DA, Zhong N, Zhang T. 2021. Sterilizing effects of novel
348 regimens containing TB47, clofazimine, and linezolid in a murine model of
349 tuberculosis. *Antimicrob Agents Chemother* 65:e0070621.

350 16. Yu W, Chiwala G, Gao Y, Liu Z, Sapkota S, Lu Z, Guo L, Khan SA, Zhong N,
351 Zhang T. 2020. TB47 and clofazimine form a highly synergistic sterilizing
352 block in a second-line regimen for tuberculosis in mice. *Biomed Pharmacother*
353 131:110782.

354 17. Yu W, Ju Y, Han X, Tian X, Ding J, Wang S, Gao Y, Li L, Li Y, Zhong N,

355 Zhang T. Bactericidal and sterilizing activity of sudapyridine-clofazimine-
356 TB47 combined with linezolid or pyrazinamide in a murine model of
357 tuberculosis. *Antimicrob Agents and Chemother* (Revised and submitted,
358 AAC00124-24R2).

359 18. Grant SS, Kawate T, Nag PP, Silvis MR, Gordon K, Stanley SA, Kazyanskaya
360 E, Nietupski R, Golas A, Fitzgerald M, Cho S, Franzblau SG, Hung DT. 2013.
361 Identification of novel inhibitors of nonreplicating *Mycobacterium*
362 *tuberculosis* using a carbon starvation model. *ACS Chem Biol* 8:2224-2234.

363 19. Wilburn KM, Fieweger RA, VanderVen BC. 2018. Cholesterol and fatty acids
364 grease the wheels of *Mycobacterium tuberculosis* pathogenesis. *Pathog Dis*
365 76:fty021.

366 20. Yang F, Njire MM, Liu J, Wu T, Wang B, Liu T, Cao Y, Liu Z, Wan J, Tu Z,
367 Tan Y, Tan S, Zhang T. 2015. Engineering more stable, selectable marker-free
368 autoluminescent mycobacteria by one step. *PLoS One* 10:e0119341.

369 21. Hu Y, Coates ARM, Mitchison DA. 2003. Sterilizing activities of
370 fluoroquinolones against rifampin-tolerant populations of *Mycobacterium*
371 *tuberculosis*. *Antimicrob Agents Chemother* 47:653-657.

372 22. Stover CK, Warrener P, VanDevanter DR, Sherman DR, Arain TM, Langhorne
373 MH, Anderson SW, Towell JA, Yuan Y, McMurray DN, Kreiswirth BN, Barry
374 CE, Baker WR. 2000. A small-molecule nitroimidazopyran drug candidate for
375 the treatment of tuberculosis. *Nature* 405:962-966.

376 23. Wayne LG, Sramek HA. 1994. Metronidazole is bactericidal to dormant cells
377 of *Mycobacterium tuberculosis*. *Antimicrob Agents Chemother* 38:2054-2058.

378 24. Commandeur S, Iakobachvili N, Sparrius M, Nur MM, Mukamolova GV,
379 Bitter W. 2020. Zebrafish embryo model for assessment of drug efficacy on

380 mycobacterial persisters. *Antimicrob Agents Chemother* 64:e00801-20.

381 25. Zhang Y, Wang S, Chen X, Cui P, Chen J, Zhang W. 2024. Mutations in the
382 promoter region of methionine transporter gene metM (Rv3253c) confer para-
383 aminosalicylic acid (PAS) resistance in *Mycobacterium tuberculosis*. *mBio*
384 15:e0207323.

385 26. Wei W, Yan H, Zhao J, Li H, Li Z, Guo H, Wang X, Zhou Y, Zhang X, Zeng J,
386 Chen T, Zhou L. 2019. Multi-omics comparisons of p-aminosalicylic acid
387 (PAS) resistance in folC mutated and un-mutated *Mycobacterium tuberculosis*
388 strains. *Emerg Microbes Infect* 8:248-261.

389 27. Zhang Y, Shi W, Zhang W, Mitchison D. 2014. Mechanisms of pyrazinamide
390 action and resistance. *Microbiol Spectr* 2:MGM2-0023-2013.

391 28. Grosset JH, Tyagi S, Almeida DV, Converse PJ, Li S-Y, Ammerman NC,
392 Bishai WR, Enarson D, Trébucq A. 2013. Assessment of clofazimine activity
393 in a second-line regimen for tuberculosis in mice. *American Journal of
394 Respiratory and Critical Care Medicine* 188:608-612.

395 29. Sumitani M, Takagi S, Tanamura Y, Inoue H. 2004. Oxygen indicator
396 composed of an organic/inorganic hybrid compound of methylene blue,
397 reductant, surfactant and saponite. *Analytical Sciences : the International
398 Journal of the Japan Society For Analytical Chemistry* 20:1153-1157.

399 30. Klementiev AD, Whiteley M. 2022. Development of a Versatile, Low-Cost
400 Electrochemical System to Study Biofilm Redox Activity at the Micron Scale.
401 *Applied and Environmental Microbiology* 88:e0043422.

402 31. Liu P, Yang Y, Tang Y, Yang T, Sang Z, Liu Z, Zhang T, Luo Y. 2019. Design
403 and synthesis of novel pyrimidine derivatives as potent antitubercular agents.
404 *European Journal of Medicinal Chemistry* 163:169-182.

405

406 **Table 1. The MICs of clinical drugs against AlRa under aerobic and anaerobic**
 407 **conditions using various media.**

Class/Targets	Drugs *	MIC ($\mu\text{g/mL}$)/aerobic conditions		MIC ($\mu\text{g/mL}$)/anaerobic conditions	
		Glycerol	Cholesterol	Glycerol	Cholesterol
Cell Wall	EMB	2	4	>64	>64
	INH	0.125	0.125	>64	>64
	VAN	16-32	16-32	>64	>64
RNA polymerase	ETH	64	64	>64	>64
	RIF	0.0625	0.0625-0.125	0.125-0.5	0.25-2
	RFB	0.008	0.008	0.03125-0.125	0.03125-0.0625
Ribosome	AMK	0.25-1	0.25-0.5	1-8	2-16
	STR	0.25-0.5	0.25-0.5	1-8	2-16
Unknown	POA	400	400	>800	>800
DNA gyrases	MOX	0.0625-0.25	0.125	0.125-2	8-32
	LEV	0.125-0.5	0.25-1	>64	>64
Respiration/ Production of NO	PA-824	0.0625	0.0625-0.125	1-4	1-4
Folic acid synthesis	SMX	> 64	> 64	>64	>64
	PAS	0.25-1	> 64	>64	>64
Respiration/ Electron transport chain	TB47	0.004-0.008	0.004-0.008	0.125-0.25	0.0625-0.25
Respiration/ ATP synthesis	BDQ	0.5-1	1-2	4-8	4-16
Unknown	CLO	0.5-1	1-2	2-8	8-16

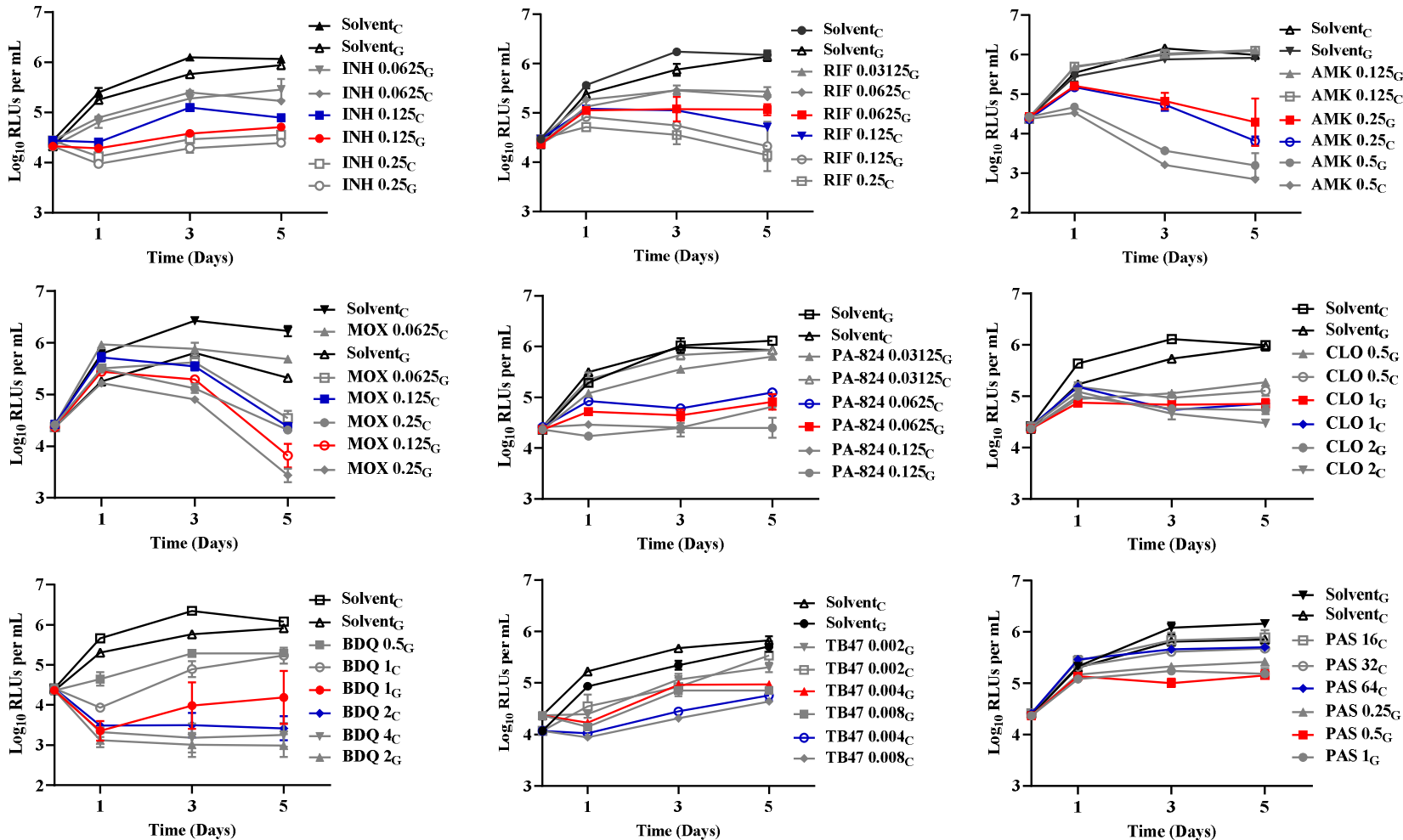
408 *EMB, ethambutol; INH, isoniazid; VAN, vancomycin; ETH, ethionamide; RIF,

409 rifampin; RFB, rifabutin; AMK, amikacin; STR, streptomycin; MOX, moxifloxacin;

410 LEV, levofloxacin; PA-824, pretomanid; SMX, sulfamethoxazole; PAS, para-

411 aminosalicylic; BDQ, bedaquiline; CLO, clofazimine.

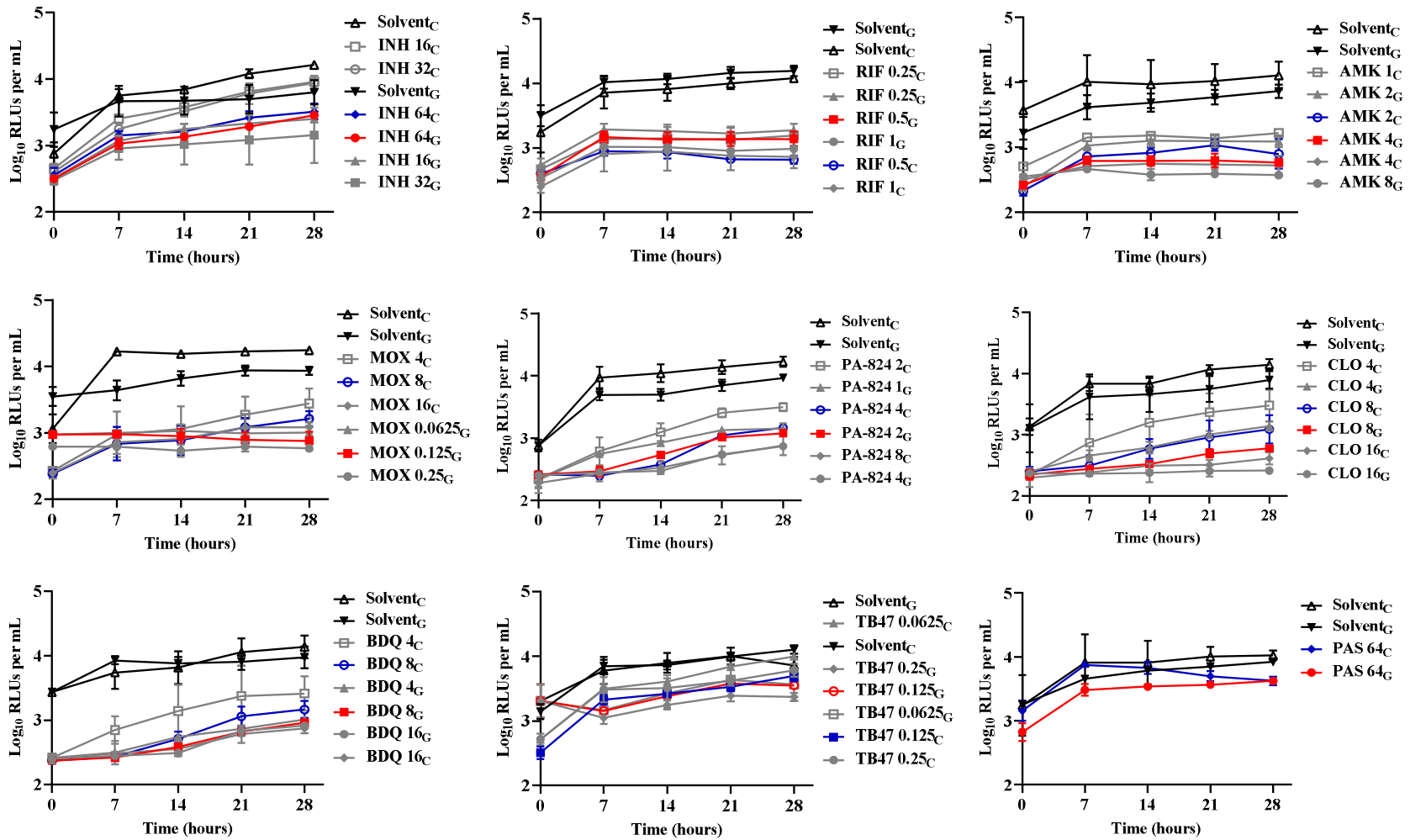
412



414 **Figure 1. The time-killing curves of actively growing *M. tuberculosis* treated with nine distinct pharmacological categories of drugs**
415 **under aerobic condition using various media.**

416 Solvent, DMSO or distilled water; G, 7H9 supplied with glycerol; C, 7H9 enriched with cholesterol; INH, isoniazid; RIF, rifampin; AMK,
417 amikacin; MOX, moxifloxacin; PA-824, pretomanid; PAS, para-aminosalicylic; BDQ, bedaquiline; CLO, clofazimine.

418



420 **Figure 2. The growth curves of nonreplicating *M. tuberculosis* after treatment with nine distinct pharmacological categories of drugs,**
421 **using various media under anaerobic condition.**

422 Solvent, DMSO or distilled water; G, 7H9 supplied with glycerol; C, 7H9 enriched with cholesterol; INH, isoniazid; RIF, rifampin; AMK,
423 amikacin; MOX, moxifloxacin; PA-824, pretomanid; PAS, para-aminosalicylic; BDQ, bedaquiline; CLO, clofazimine.

424

425 **Table 2. MICs of CLO and TB47 against AlRa along with the corresponding**
426 **interaction profiles of CLO in conjunction with TB47 assessed by checkerboard**
427 **method under anaerobic condition.**

Drugs [*]	7H9 + Glycerol		7H9 + Cholesterol	
	MIC _a [#]	MIC _c [#]	MIC _a [#]	MIC _c [#]
TB47	0.125	0.03125	0.125	0.03125
CLO	8	4	8	4
FICI [□] / Effect	0.75 / partially synergistic	0.75 / partially synergistic		

428 ^{*}CLO, clofazimine.

429 [□]FICI, Fractional inhibitory concentration index; The FICI was calculated as the ratio
430 of the MIC of TB47 in combination to the MIC of TB47 alone, plus the MIC of CLO
431 in combination to the MIC of CLO alone. The FICI was calculated to classify the
432 interactions as one of five kinds: synergistic (FICI ≤ 0.5), partially synergistic ($0.5 <$
433 FICI < 1.0), additive (FICI = 1.0), indifferent ($1.0 < \text{FICI} \leq 4.0$) or antagonistic (FICI $>$
434 4.0) (31).

435 [#]MIC_a, MIC alone; MIC_c, MIC in combination.

436

437

438